Cell

Asymmetric Inheritance of Centrosome-Associated Primary Cilium Membrane Directs Ciliogenesis after Cell Division

Judith T.M.L. Paridaen,[1] Michaela Wilsch-Bräuninger,[1] and Wieland B. Huttner[1,*]
[1]Max Planck Institute of Molecular Cell Biology and Genetics, Pfotenhauerstraβe 108, 01307 Dresden, Germany
*Correspondence: huttner@mpi-cbg.de
http://dx.doi.org/10.1016/j.cell.2013.08.060

SUMMARY

Primary cilia are key sensory organelles that are thought to be disassembled prior to mitosis. Inheritance of the mother centriole, which nucleates the primary cilium, in relation to asymmetric daughter cell behavior has previously been studied. However, the fate of the ciliary membrane upon cell division is unknown. Here, we followed the ciliary membrane in dividing embryonic neocortical stem cells and cultured cells. Ciliary membrane attached to the mother centriole was endocytosed at mitosis onset, persisted through mitosis at one spindle pole, and was asymmetrically inherited by one daughter cell, which retained stem cell character. This daughter re-established a primary cilium harboring an activated signal transducer earlier than the noninheriting daughter. Centrosomal association of ciliary membrane in dividing neural stem cells decreased at late neurogenesis when these cells differentiate. Our data imply that centrosome-associated ciliary membrane acts as a determinant for the temporal-spatial control of ciliogenesis.

INTRODUCTION

The primary cilium is an antenna-like projection of the cell that consists of nine microtubule doublets surrounded by ciliary membrane (CM). The primary cilium is nucleated at its base by the basal body, consisting of the eldest centriole in the cell—the mother centriole—with associated appendage proteins that dock it to the plasma membrane (Garcia-Gonzalo and Reiter, 2012; Kim and Dynlacht, 2013; Seeley and Nachury, 2010). Although the CM is continuous with the plasma membrane, entry of membrane proteins into the cilium is restricted (Nachury et al., 2010; Reiter et al., 2012). Thus, the primary cilium forms a separate cell compartment, providing a platform for several extracellular signals, such as Sonic Hedgehog (Shh), an important regulator of proliferation and embryonic patterning (Goetz and Anderson, 2010).

A generally accepted concept is that primary cilia are disassembled prior to mitosis so that the centrioles can function at the poles of the mitotic spindle (Garcia-Gonzalo and Reiter, 2012; Kim and Dynlacht, 2013; Kim and Tsiokas, 2011; Seeley and Nachury, 2010). At the end of cell division, the daughter centriole of the previous cell cycle matures into a new mother centriole and will, as the old mother centriole, nucleate a new cilium in early G1 (Nigg and Stearns, 2011).

In the developing neocortex, a primary cilium extends from the apical membrane of epithelial neural stem cells, called apical progenitors (APs), into the lateral ventricle (Louvi and Grove, 2011). Here, the cilium is able to detect signals present in the cerebrospinal fluid (CSF) (Lehtinen and Walsh, 2011). Upon onset of neurogenesis, APs switch from symmetric proliferative divisions to mainly asymmetric neurogenic divisions (Götz and Huttner, 2005; Kriegstein and Alvarez-Buylla, 2009; Lancaster and Knoblich, 2012). These APs produce neurons either directly or via fate-restricted basal progenitors that delaminate from the ventricular surface.

Asymmetric inheritance of the centrosome containing the mother centriole into one daughter cell is linked to maintenance of stem cell character in the *Drosophila* germline and the developing mouse neocortex (Pelletier and Yamashita, 2012, Yamashita et al., 2007, Wang et al., 2009). In addition, in cultured cells, the daughter cell that inherits the mother centriole reassembles a cilium earlier than its sister cell (Anderson and Stearns, 2009). Asynchronous cilium reformation was also observed in AP divisions in the mouse neural tube by live imaging (Piotrowska-Nitsche and Caspary, 2012). This asynchrony differentially exposes the daughter cells to primary cilium-transmitted signals (Anderson and Stearns, 2009; Piotrowska-Nitsche and Caspary, 2012).

These studies support the notion that inheritance of centrosome-associated structures is involved in asymmetric regulation of cell fate between daughter cells. The fate of one such structure, the CM, upon entry into mitosis is currently unknown. Here, we have investigated the fate of the CM upon division of mouse embryonic neocortical stem cells and cells in culture. Our findings indicate that, contrary to previous concepts, primary cilia are not completely disassembled prior to mitosis. Our study uncovers a yet unknown feature of cell division with relevance for asymmetric daughter cell behavior that explains the previously reported asynchrony in cilium re-establishment and signaling between daughter cells.

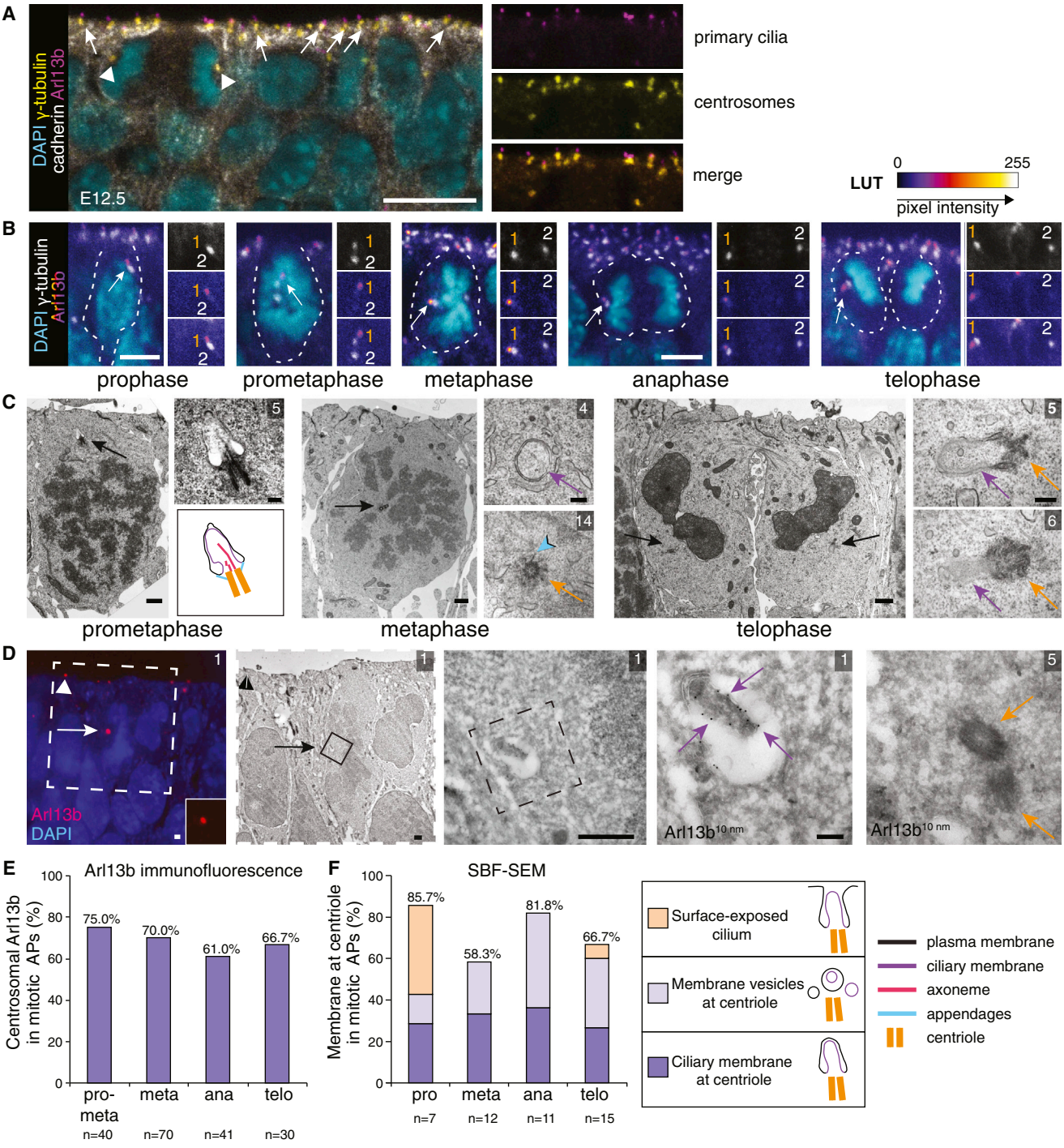

Figure 1. The Ciliary GTPase Arl13b Is Associated with One of the Centrosomes in Mitotic APs

(A) Confocal image of immunofluorescence for Arl13b (magenta) and γ-tubulin (yellow) to outline primary cilia and the centrosome (long arrows) in APs in the E12.5 mouse dorsal telencephalon. Pan-cadherin (gray) marks junctions and lateral plasma membrane, and nuclei are stained with DAPI (cyan). Arrowheads indicate the two centrosomes in a single mitotic AP. Insets to the right show single fluorescence and merged channels.

(B) Confocal images of single APs in progressive phases of mitosis (DAPI, cyan) show association of Arl13b protein (arrows; magenta, lookup table [LUT]) with one of the centrosomes (γ-tubulin, gray). A "fire" LUT was used to show Arl13b signal intensities. Insets show cropped single and merged channels. Dashed lines outline single mitotic APs. (A and B) All images are maximum projections with optical sections of 0.5 μm.

(C) Transmission electron micrographs of single mitotic APs from E12.5 dorsal telencephalon at progressive stages of mitosis showing membrane near a centriole (black arrows). In the insets, magnifications of the CM (purple arrows), distal appendages (cyan arrowhead), and centriole (orange arrows) and a schematic drawing of the CR are presented. Number indicates the serial section number; see Figure S1 for all serial sections.

(legend continued on next page)

RESULTS

A Membrane Vesicle Containing the Ciliary GTPase Arl13b Is Associated with the Centrosome in Mitotic Apical Progenitors

The small GTPase ADP-ribosylation factor-like 13b (Arl13b) specifically associates with the CM via a palmitoyl moiety (Cevik et al., 2010; Duldulao et al., 2009; Horner and Caspary, 2011). As described previously, we found that Arl13b marks primary cilia protruding from the apical membrane of APs in the developing mouse cortex (Figure 1A). In mitotic APs, we detected Arl13b protein near one of the centrosomes of the spindle (Figure 1B). This centrosomal localization of Arl13b was observed throughout mitosis in most dividing APs (Figures 1B and 1E).

We used electron microscopy (EM) to analyze the structural basis of this subcellular Arl13b localization. Using conventional transmission EM analysis (Figure 1C and Figure S1 available online) as well as serial-block-face scanning EM (SBF-SEM; Figure 1F), we identified membraneous structures in close association with one centriole of one spindle pole in the majority of mitotic APs. These membrane structures characteristically appeared as membranes enclosed by, or budding into, a larger membrane vesicle (Figures 1C and S1). Moreover, the inner membrane appeared to be anchored to the centriole via appendages similar to transitional fibers docking the basal body in interphase cells to the plasma membrane, suggesting that these structures constitute an intracellular ciliary remnant (CR) (Figure S1). Indeed, the Arl13b-positive (Arl13b$^+$) puncta seen in immunofluorescence were observed to correspond to centriole-attached immunogold-labeled membrane structures (Figure 1D). Arl13b was mainly localized to the inner membrane of these structures (Figures S2A–S2E). In some cases, the Arl13b$^+$ membrane appeared fragmented within the outer, surrounding membrane (Figure S2E). We did not observe specific Arl13b immunoreactivity directly on centrioles. Importantly, the frequency of centriole-associated membranes in mitotic APs as detected by SBF-SEM (Figure 1F) was comparable to that of centrosome-associated Arl13b as detected by immunofluorescence (Figure 1E). Taken together, these data show that, in most mitotic APs, an intracellular Arl13b$^+$ CM is attached to a centriole via appendages similar to those found in interphase cilia.

The Arl13b$^+$ Ciliary Membrane Is Derived from the Apical Primary Cilium

To corroborate the ciliary identity of the Arl13b$^+$ membrane, we made use of two well-known ciliary transmembrane proteins, namely, the somatostatin receptor 3 (Sstr3) and the serotonin (5-hydroxytryptamine) receptor 5HT6 (Berbari et al., 2008). We electroporated DNA constructs encoding EGFP-tagged versions of these proteins into the developing mouse dorsolateral telencephalon at E12.5 and analyzed dividing APs at E13.5.

As expected, Sstr3-EGFP localized specifically to the cilia of APs at interphase (Figure 2A). In mitotic APs, Sstr3-EGFP was localized close to one of the centrosomes and seemed to enclose the Arl13b$^+$ dot (Figure 2B). A similar localization was observed for 5HT6-EGFP (data not shown). These results strengthen our conclusion that the Arl13b$^+$ membrane has ciliary identity.

We next investigated whether the Arl13b$^+$ membrane represents de novo synthesized CM or an internalized membrane-containing remnant of the primary cilium present during interphase. To explore the latter, we analyzed whether the Arl13b$^+$ dot contains CM that was internalized from the cell surface at the onset of mitosis. We adopted a cell-surface biotinylation approach that has previously been widely used in endocytosis and recycling studies (Figure 2C). The apical surface of the telencephalon was biotinylated at 4°C using the membrane-impermeable Sulfo-NHS-SS-biotin (Figure 2C). Control samples kept at 4°C to prevent membrane internalization showed biotinylation (as detected by fluorescent streptavidin) of the apical membrane and CM of APs (Figures 2D, S3A, and S3B). No biotinylated membrane was detected at the centrosome of mitotic APs in the control samples (Figures 2D, 2G, S3C, S3D, and S3F). In contrast, analysis of mitotic APs in samples that were chased at 37°C for up to 3 hr showed the presence of multiple intracellular biotinylated membrane dots. Only one of these overlapped with the intracellular centrosome-associated Arl13b$^+$ membrane (Figures 2E, 2F, 2H, 2I, and S3H). These results show that the latter membrane had been internalized from the cell surface.

Further support for this conclusion was obtained by SBF-SEM. This revealed an entire primary cilium in a deep plasma membrane invagination of an AP at the G2-M phase transition, apparently undergoing endocytosis (Movie S1).

The Ciliary Membrane Remains Associated with the Basal Body throughout Mitosis

The above data suggest that, in contrast to the generally accepted concept that primary cilia are completely disassembled for mitosis, the CM remains attached to the basal body throughout mitosis. To further corroborate this, we examined the localization of the CM relative to the mature centriole-specific proteins Cep164 (Graser et al., 2007; Sillibourne et al., 2011) and ninein (Mogensen et al., 2000) in mitotic APs. Cep164 localizes at the basal body distal appendages that

(D) Arl13b immunolocalization in correlative light (left; red) and electron (second to left to right; 10 nm immunogold) microscopy of an E12.5 metaphase AP. In the LM image, the nucleus is counterstained with DAPI (blue). Boxed region in the second image is magnified in the middle panel. Right two panels are magnifications of the boxed region (middle panel) in two serial sections (number of the section indicated). Arl13b$^+$ apical primary cilia (arrowheads) and CM (white, black and purple arrows), as well as the centrioles (orange arrows) are indicated.

(E) Quantitation of the percentage of mitotic APs showing centrosome-associated Arl13b on immunofluorescence at progressive stages of mitosis at E12.5. Data extracted from Figure 5C.

(F) Quantitation of the percentage of mitotic APs showing CM or membrane vesicles (dark or light purple) directly associated with a centriole, and surface-exposed cilia (yellow), on SBF-SEM at progressive stages of mitosis at E12.5.

Scale bars, 10 μm (A), 5 μm (B), and 1 μm (C and D) for overview pictures; 200 nm for magnifications. See also Figures S1, S2, and Movie S1.

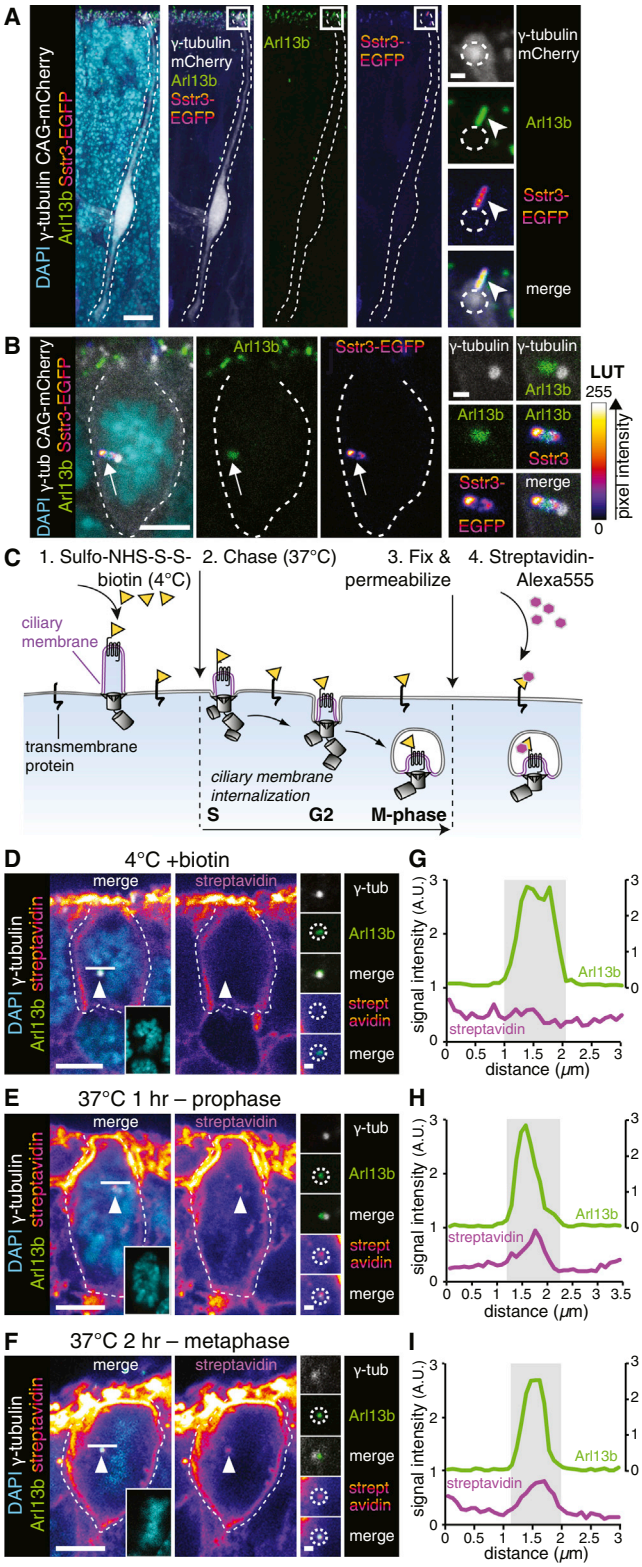

Figure 2. The Arl13b$^+$ Membrane Dot Constitutes an Internalized Ciliary Remnant

(A and B) Confocal images of E13.5 mouse dorsal telencephalon with a single AP (outlined by dashed lines) in interphase (A) or mitosis (B; n = 42), expressing Sstr3-EGFP (magenta, LUT) and CAG-mCherry (gray). Nuclei are labeled with DAPI (cyan), and γ-tubulin (gray) and Arl13b (green) identify centrosomes and CM (arrows in B), respectively. A "fire" LUT that visualizes pixel intensity is used for Sstr3-EGFP. (A) Boxed region is magnified in the right panels. Dashed circles in insets indicate position of the centrosome. Arrowheads indicate the primary cilium. Maximum projection with 0.4 μm optical sections. (B) Single optical sections of 0.4 μm. Magnifications on the right show single fluorescence and merged images.

(C) Experimental setup for cell-surface biotinylation and chase of APs.

(D–F) Confocal images of single mitotic APs (outlined by dashed lines) in control samples incubated with biotin at 4°C (D; n = 12 mitotic APs) or in chased samples cultured at 37°C after biotinylation (E and F; n = 24 mitotic APs). Images show (immuno)fluorescence for γ-tubulin (gray), Arl13b (green), and streptavidin (magenta, LUT), with nuclei stained with DAPI (single DAPI channel in insets). A "fire" LUT that visualizes pixel intensity is used for streptavidin. CM is indicated by arrowheads in the overview pictures and dashed circles in the insets. Insets show single immunofluorescence and merged images. Images are single 0.4 μm optical sections.

(G–I) Fluorescence intensity plot profiles of Arl13b and streptavidin signals along the white lines in (D–F). Arl13b signal plot was repositioned and rescaled on the y axis to facilitate visualization. Gray boxes indicate the limits of the Arl13b fluorescence signal.

Scale bars, 10 μm (A), 5 μm (B and D–F), and 1 μm (insets in A, B, and D–F). See also Figure S3.

anchor cilia in interphase cells (Graser et al., 2007; Sillibourne et al., 2011). Ninein localizes at the subdistal appendages of the mother centriole as well as the proximal end of both mother and daughter centrioles (Mogensen et al., 2000). Cep164 and ninein are retained at the older mother centriole during mitosis (Graser et al., 2007; Mogensen et al., 2000). Furthermore, the original daughter centriole slowly accumulates these proteins as it matures into a new mother centriole during mitosis.

As expected, EGFP-tagged Cep164 and ninein were localized at the distal end of the basal body (Figures 3A, left, and 3C, left). Consistent with previous reports (Graser et al., 2007; Mogensen et al., 2000), EGFP-Cep164 and EGFP-ninein showed a difference in signal intensity between the two poles of the mitotic spindle (Figures 3A, middle and right, 3B, 3C, right, 3D, and 3E). As this signal difference very likely reflects the different age of the centrioles, we assume that the centrosome containing the highest levels of Cep164 and ninein contains the older mother centriole. Arl13b immunofluorescence showed that the intracellular Arl13b$^+$ CM was associated with the older mother centriole in the majority of mitotic APs (Figures 3A, middle and right, 3B, 3C, right, 3D, and 3F). Together with the EM observations (Figures 1C and S1), these data indicate that the attachment of the CM to the basal body through the distal appendages is maintained during mitosis.

Asymmetric Inheritance of the Ciliary Remnant by Daughter Cells Is Linked to Early Cilium Reassembly in Cell Lines

We next investigated whether persistence of centrosome-associated CM during mitosis is present in cell types other than APs. To this end, we analyzed Arl13b localization in human embryonic kidney (HEK293T) and mouse neuroblastoma (Neuro2a) cells. About 25% of HEK293T cells carried an Arl13b$^+$ primary cilium in interphase (Figures 4A and 4B). Similarly, about 25% of mitotic HEK293T cells showed Arl13b immunofluorescence near one

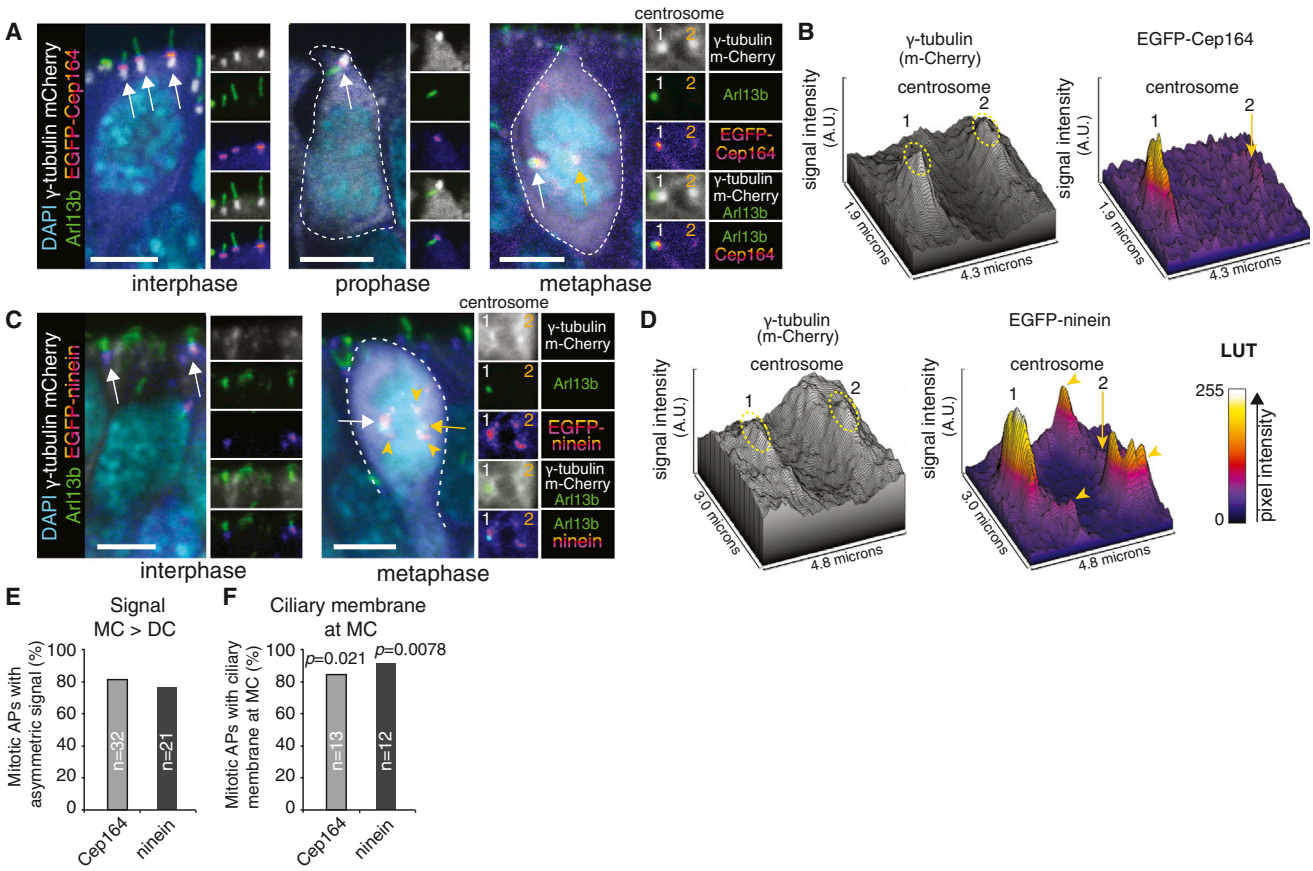

Figure 3. The Ciliary Membrane Remains Associated with the Mother Centriole-Containing Centrosome during Mitosis

(A) Confocal images of E13.5 APs expressing EGFP-Cep164 (magenta, LUT) and CAG-mCherry (gray). A "fire" LUT that visualizes pixel intensity is used for EGFP-Cep164. Images show immunofluorescence for γ-tubulin (gray) and Arl13b (green), with nuclei stained with DAPI (cyan), in interphase (left) and mitotic (middle and right) APs. White arrows indicate primary cilia (left) or CM at centrosome 1 (middle and right). Yellow arrow indicates centrosome 2. Insets show single and merged channel images. (left, middle) Maximum projection; (right) sum slices projection.

(B) Fluorescence signal intensity profiles of γ-tubulin (left) and EGFP-Cep164 (right) for centrosome 1 and 2 (yellow dashed circles) as indicated in (A, right).

(C) Confocal images of E13.5 APs expressing EGFP-ninein (magenta, LUT) and CAG-mCherry (gray). Images show immunofluorescence for γ-tubulin (gray) and Arl13b (green), with nuclei stained with DAPI (cyan), in interphase (left) and mitotic (right) APs. A "fire" LUT that visualizes pixel intensity is used for EGFP-ninein. Yellow arrowheads indicate EGFP-ninein localized at microtubules (C right, D right). White arrows indicate primary cilia (left) or CM at centrosome 1 (right). Yellow arrow indicates centrosome 2. Insets show single and merged channel images. (Left) Maximum projection; (right) sum slices projection.

(D) Fluorescence signal intensity profiles of γ-tubulin immunofluorescence (left) and EGFP-ninein signal (right) for centrosome 1 and 2 (yellow dashed circles) as indicated in (C right).

(E) Quantification of the percentage of mitotic cells that showed a difference in average signal intensity (>25%) for EGFP-Cep164 and EGFP-ninein between the centrosomes.

(F) Quantification of the percentage of cells showing association of the CM with the mother centriole over the total number of analyzed mitotic cells. A two-tailed exact binomial probability test was performed with p values indicated. (E and F) MC, mother centriole; DC, daughter centriole.

Scale bars, 5 μm (A and C).

centrosome (Figures 4B and 4C). EM immunolocalization confirmed the presence of Arl13b$^+$ CM in close vicinity to a centriole (Figures S2F and S2G), similar to what was observed in mitotic APs (Figures S2A–S2E). Similar findings were obtained by Arl13b immunofluorescence of Neuro2a cells (data not shown). These results indicate that the occurrence of a CR in mitotic cells is not limited to embryonic neural stem cells but occurs in a variety of cell types.

Previous studies have demonstrated a link between old mother centriole inheritance and asynchronous cilium reformation (Anderson and Stearns, 2009; Piotrowska-Nitsche and Caspary, 2012). Therefore, we investigated inheritance of the CR and the timing of cilium reformation in pairs of daughter cells by live imaging (Figures 4D and S4; Movie S2).

Imaging of interphase HEK293T cells showed shortening of the cilium (monitored using fluorescent protein-tagged Arl13b) prior to entry into mitosis (Figure 4D; Movie S2). Upon entry into mitosis, the CM was internalized together with one of the centrosomes (Figure S5A). This CR was asymmetrically inherited by one daughter cell in most divisions (Figures 4D, 4E, S4, and S5A; Movie S2). Subsequently, a cilium was reformed within a few hours in this daughter cell (daughter cell 1; Figures 4D–4F, S4,

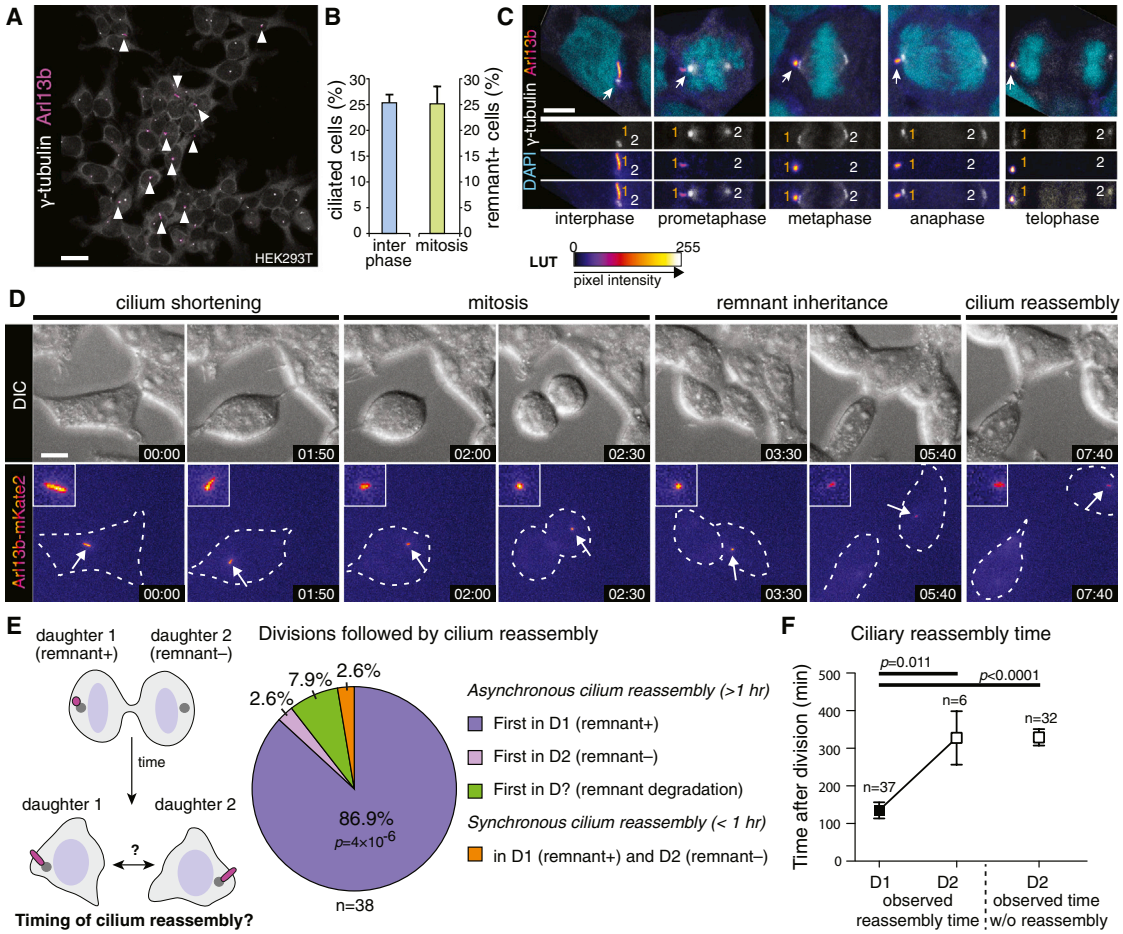

Figure 4. Asymmetric Inheritance of the Ciliary Remnant Is Linked to Early Cilium Reassembly in HEK293T Cells

(A) Overview confocal image showing Arl13b^{+} (magenta) primary cilia (arrowheads) and γ-tubulin (gray) immunofluorescence of HEK293T cells.

(B) Quantification of the percentage of ciliated cells over total interphase cells (left; n = 2211 total cells) and of the percentage of mitotic cells containing a CR (right; n = 221 mitotic cells). Error bars represent SD.

(C) Confocal images of mitotic HEK293T cells showing Arl13b (magenta, LUT) and γ-tubulin (gray) immunofluorescence, with nuclei counterstained with DAPI (cyan). A "fire" LUT was used to visualize Arl13b signal intensity. Arrows indicate CM. Insets show single and merged channels. The centrosomes are numbered. All images are maximum projections with single z plane of 0.4 μm.

(D) Still images (maximum projection) from time-lapse live imaging of HEK293T cells transfected with pArl13b-mKate2. Top row shows DIC images at the indicated time points (hours:minutes). Bottom row shows CM (arrows) revealed by Arl13b-mKate2 (magenta, LUT). Dashed lines indicate the outline of the dividing cell. Insets show magnifications of the CM.

(E) Quantification of all mitoses that were followed by cilium reassembly within the time of observation. D1 is defined as the CM-inheriting daughter cell 1; D2 is defined as the daughter cell 2 that did not inherit the CM. Asynchronous versus synchronous reformation is defined as >1 hr or <1 hr difference, respectively, in ciliary reassembly between the daughter cells. A two-tailed exact binomial probability test was performed with the p value indicated. For raw data, see Figure S4.

(F) Quantification of the ciliary reassembly times or the total time of observation without cilium reassembly. Data are represented as mean ± SEM, with the number of daughter cells indicated. For raw data, see Figure S4. A two-tailed Mann-Whitney test was performed with p values indicated. DIC, differential interference contrast; LUT, lookup table.

Scale bars, 10 μm (A and D) and 5 μm (C). See also Figures S1, S4, S5, and Movie S2.

and S5A; Movie S2). In contrast, only a few daughter cells that had not inherited the CR (daughter cell 2) showed cilium reformation within the time of observation (Figures 4D–4F and S4), suggesting that these cells formed a cilium either much later or not at all. Comparison of the ciliary reassembly times between CR-inheriting versus noninheriting daughter cells showed that ciliary reformation occurred earlier in the former (Figure 4F). We obtained similar observations by live imaging of Neuro2a cells (data not shown). In addition, we corroborated the Arl13b live imaging observations by using Sstr3-EGFP as another marker of the CM in dividing HEK293T cells (Figure S5B). Together, these data demonstrate that inheritance of the CR is linked to earlier reassembly of the cilium in early G1 phase after mitosis.

Asymmetric Ciliary Remnant Inheritance Peaks during Early Neurogenesis

At the onset of neurogenesis, APs switch from symmetric to asymmetric divisions. We wondered whether asymmetric CR

inheritance is a hallmark of dividing APs at both preneurogenic and neurogenic stages. Therefore, we examined the localization of Arl13b relative to the centrosomes in mitotic APs at several developmental stages (Figure 5). Prior to the onset of neurogenesis, as well as during early neurogenesis, Arl13b was localized near one centrosome in most APs (Figures 5A, top-right panel; 5B, 5C, and 5F, purple). Moreover, a subset of mitotic APs showed weak Arl13b staining next to the second centrosome as well (Figures 5A, bottom-right panel, 5B, 5C, and 5F, red).

In contrast, at later neurogenic stages, most mitotic APs showed Arl13b localization at some distance from either centrosome (Figures 5A, bottom-left panel, 5D–5F, yellow). Upon surface biotinylation and chase, we observed that this noncentrosomal form of CM in mitotic APs contains biotinylated membrane derived from the surface of the cell (Figures S3E and S3G), similar to centrosome-associated CM. Together, these data show that persistence of the CR throughout mitosis occurs most frequently at preneurogenic and early neurogenic stages. In addition, they suggest that, as neurogenesis progresses, the CM can lose its attachment to the old mother centriole during mitosis.

Ciliary Remnant Inheritance Underlies Early Cilium Reassembly in Primary Neural Stem Cells

We next investigated the asymmetric inheritance of the CR in AP divisions by live imaging of organotypic slices of, and acutely dissociated cells derived from, dorsolateral telencephalon (Figures 6A–6C). Prior to imaging, APs were electroporated in utero with a combination of ciliary, centrosomal, and membrane markers. In organotypic slices, we observed that the Arl13b$^+$ CM was internalized at the G2-M phase transition, persisted intracellularly through mitosis, and was asymmetrically inherited by one daughter cell (Figure 6A).

In order to study the relationship between CR inheritance and the timing of cilium reassembly in greater detail, we monitored divisions of single dissociated APs and their progeny (Figures 6B–6F and S6A). First, we found that, similar to what we had observed in fixed tissue (Figure 5), half of the dividing APs showed asymmetric CR inheritance by one daughter at early neurogenesis (E12.5; Figures 6B and 6D, left, purple; Movie S3). The other APs showed (1) cilium disassembly followed by CM degradation prior to the onset of mitosis, as suggested by the loss of the Arl13b signal (Figure 6D, left, blue) or, in a few cases, either (2) CM degradation during mitosis (Figures 6C and 6D, left, green; Movie S4), or (3) dissociation of the CM from the centrosome during mitosis followed by inheritance by one daughter cell (Figure 6D, left, yellow; Movie S5). At later stages of neurogenesis, fewer AP divisions showed CR inheritance (E14.5–E15.5 Figure 6D, right, purple). At the same time, an increased proportion of dividing APs showed either CM degradation (Figure 6D, right, green), or its dissociation from the centrosome (Figure 6D, right, yellow), during mitosis. Similar observations were made using Sstr3-EGFP as a marker of CM (Figure S6A).

Next, we compared cilium reformation in the daughter cells of AP divisions with or without CR inheritance (Figures 6E and S6A). In divisions with asymmetric CR inheritance, the CR-inheriting daughter cell reformed a cilium significantly earlier than its

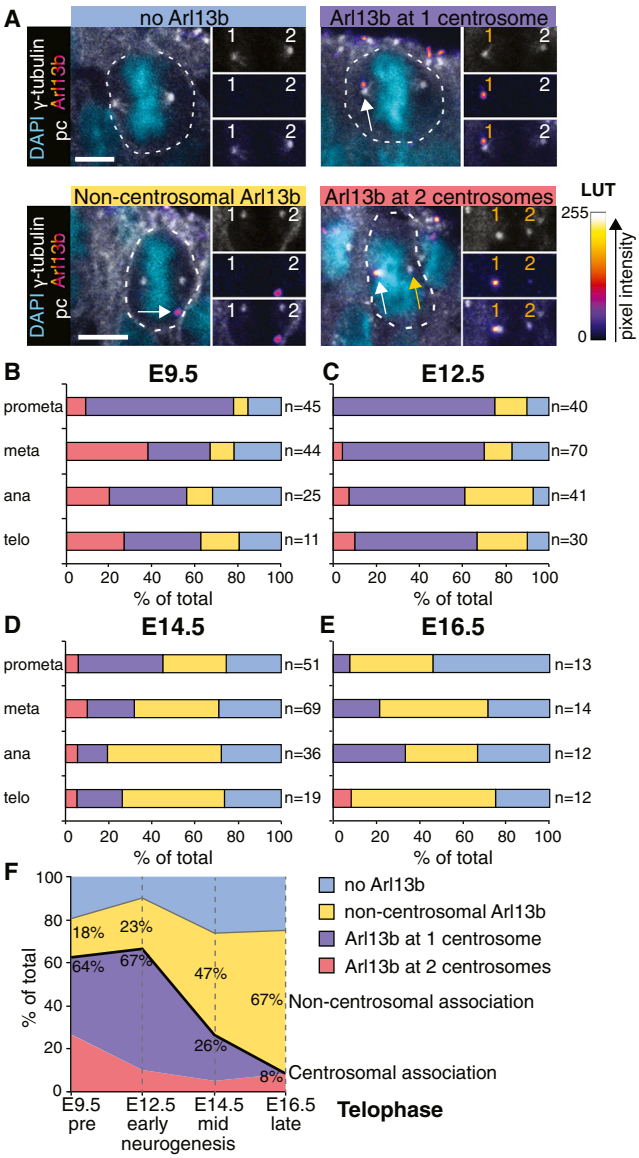

Figure 5. Centrosomal Association of the Ciliary Membrane in Mitotic APs Decreases during Neurogenesis

(A) Confocal images of mitotic APs at E12.5 showing immunofluorescence for Arl13b (magenta, LUT) and γ-tubulin together with pan-cadherin indicating the lateral plasma membrane (gray). A "fire" LUT was used to show Arl13b signal intensities. The Arl13b$^+$ membrane (arrows) displays three different patterns relative to the centrosome. Insets show the single and merged channels. Dashed lines outline single mitotic APs. All images are maximum projections with 0.5 μm optical sections.

(B–E) The occurrence of the Arl13b localization patterns (see A and color key) in mitotic APs at progressive stages of mitosis at E9.5 (B), E12.5 (C), E14.5 (D), and E16.5 (E) is expressed over the total number of mitotic APs analyzed.

(F) Quantification of the subcellular Arl13b localization types as percentage of total telophase APs from preneurogenesis to late neurogenesis. Black line indicates the percentage of APs showing centrosomal association (purple + red).

Scale bar, 5 μm (A).

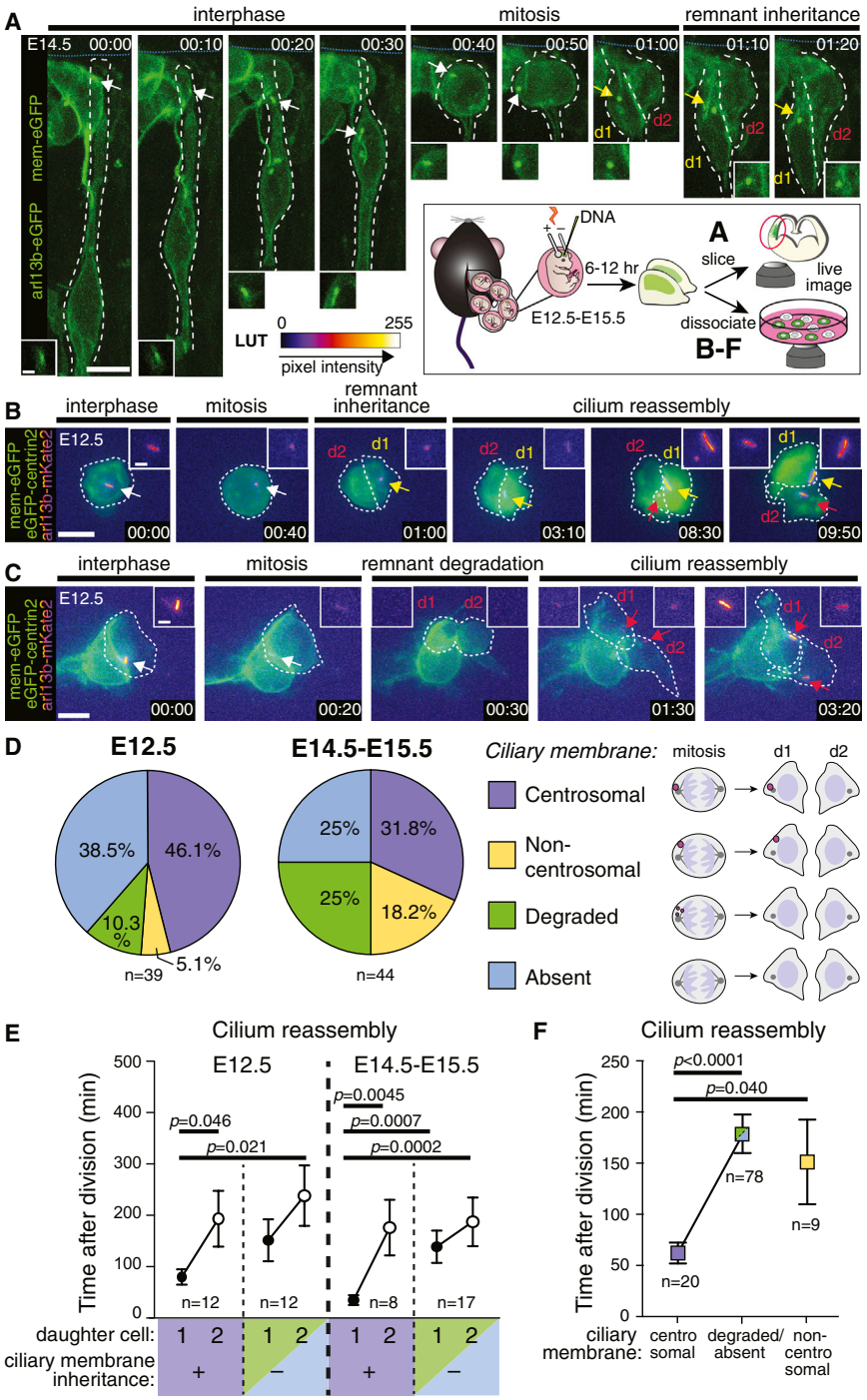

Figure 6. Live Imaging Showing Ciliary Membrane Inheritance and Asynchronous Cilium Reformation in Dividing APs

(A) Still images (maximum projection) from time-lapse live imaging of a single dividing AP in an E14.5 organotypic slice expressing GAP43-GFP (Golgi and plasma membrane; green) and EGFP-Arl13b (CM; green; white arrows). Time intervals between frames are indicated (hours:minutes). CM inheritance into daughter cell 1 is indicated by yellow arrows (n = 7). Dashed lines indicate the outline of the mitotic cell. Blue dotted lines indicate the apical surface. Insets show magnification of CM. Box: Schematic drawing showing experimental setup for (A) and (B–F).

(B and C) Still images (maximum projection) from time-lapse live imaging of acutely dissociated APs (E12.5) that express GAP43-GFP (plasma membrane; green), EGFP-centrin2 (centrioles; green), and Arl13b-mKate2 (CM; magenta LUT). A "fire" LUT was used to show Arl13b signal intensities. Time intervals between frames are indicated (hours:minutes). CM is indicated by white arrows, and its inheritance into daughter cell 1 (B) is indicated by yellow arrows. De novo assembled cilia (B and C) are indicated by red arrows. Dashed lines indicate the outline of the mitotic cells. Insets show magnification of CM.

(D) Quantification of CM localization (see color key) in mitotic dissociated APs at E12.5 (left) and E14.5–E15.5 (right).

(E) Quantification of the ciliary reassembly time and/or the total time of observation without cilium reassembly in daughter cells 1 (CR-inheriting and/or fast reassembly; black circles) and 2 (non-CR-inheriting and slow reassembly; open circles) of divisions with (purple) or without (blue/green) CR inheritance at E12.5 (left) and E14.5–E15.5 (right).

(F) Quantification of the ciliary reassembly time and/or the total time of observation without cilium reassembly in centrosomal membrane-inheriting (purple), noncentrosomal membrane-inheriting (yellow), and noninheriting (blue/green) cells. Data (purple, green/blue) are pooled from (E).

In (E) and (F), data are represented as mean ± SEM, with the number of AP divisions indicated. A two-tailed Mann-Whitney test was performed with p values indicated. d1/d2, daughter cell 1/2; LUT, lookup table; mem, membrane. Scale bars, 10 μm (A–C) and 2 μm (insets in A–C). See also Figure S6A and Movies S3, S4, and S5.

noninheriting sister cell, both at early and midneurogenic stages (Figure 6E, purple). In contrast, there was no significant difference in the timing of cilium reformation between daughter cells of divisions without CR inheritance (due to CM degradation; Figure 6E, green and blue). Comparing all CM-inheriting cells with all noninheriting cells, cilium reformation occurred about three times earlier in the former (62.2 ± 10.3 min versus 178.7 ± 18.9 min; Figure 6F). Interestingly, daughter cells inheriting non-centrosomal CM, which disappeared shortly thereafter, reformed a cilium later (151.2 ± 41.3 min; Figure 6F; Movie S5) than daughter cells that inherited a centrosomal CM.

Taken together, these data demonstrate that the asymmetric CR inheritance followed by earlier cilium reassembly occurs also in primary embryonic neural stem cells. Moreover, the findings that daughter cells without CM or with noncentrosomal CM show delayed cilium reassembly, although one of the daughters

contains the old mother centriole, indicate that inheritance of centrosome-associated CM underlies the earlier cilium reassembly.

Remnant Inheritance Underlies Early Ciliary Smoothened Accumulation

Previous studies have demonstrated that asynchronous cilium reformation is linked to differential ciliary signaling between daughter cells (Anderson and Stearns, 2009, Piotrowska-Nitsche and Caspary, 2012). We wondered whether this phenomenon is based on asymmetric inheritance of the CR. Therefore, we investigated the ciliary accumulation of the transmembrane protein Smoothened (Smo), a well-known transducer of Shh signaling (Robbins et al., 2012), in AP divisions with and without CR inheritance (Figure S6B). Upon activation of Smo, either through activation of the receptor Patched by the ligand Shh or via direct activation by a Smo agonist (SAG), Smo translocates from the plasma membrane to the CM (Chen et al., 2002; Frank-Kamenetsky et al., 2002; Rohatgi et al., 2007). Here, activated Smo can exert its downstream effects on processing of the Gli transcription factors, ultimately leading to signal transduction to the nucleus (Robbins et al., 2012).

We examined whether the asynchronous cilium reassembly preceded by CR inheritance is accompanied by asynchronous ciliary accumulation of activated Smo, using live imaging of dissociated APs expressing EGFP-tagged Smo and Arl13b-mKate, cultured in the absence (Figure 7C, left) or presence (Figures 7A–7C, right) of SAG. As expected, treatment with SAG induced ciliary accumulation of activated Smo-EGFP in interphase (Figure 7C, right).

In AP divisions with CR inheritance, some Smo-EGFP persisted as a fluorescent dot through mitosis and was asymmetrically inherited, together with the Arl13b$^+$ CM, by one daughter cell that reassembled the cilium earlier than its noninheriting sister cell (Figure 7A; Movie S6). Concomitantly, Smo-EGFP accumulated significantly earlier in the cilium of the CR-inheriting daughter cell (Figures 7A, 7D, and 7E, purple; Movie S6). In contrast, in AP divisions without CR inheritance (due to degradation of the CM during mitosis), synchronous cilium reformation and accumulation of ciliary Smo-EGFP in the two daughter cells were observed (Figures 7B, 7D, and 7E, green; Movie S7). Comparing all CR inheriting with all noninheriting daughter cells, ciliary accumulation of Smo-EGFP occurred significantly earlier in the former (80.4 ± 22.5 min versus 153.5 ± 18.8 min; Figure 7F). As ciliary Smo regulates processing of the Gli transcription factors into activator form, it is plausible that this earlier ciliary Smo accumulation may result in earlier Shh signaling activity. We conclude that inheritance of the CR underlies asymmetric ciliary signaling between daughter cells.

The Ciliary Remnant Is Preferentially Inherited by the Stem Cell Daughter Cell

Previously, it was reported that in the developing mouse neocortex, the elder centrioles are preferably inherited by the daughter cells fated to remain APs (Wang et al., 2009). We wondered whether the CM as an older mother centriole-associated structure is similarly preferentially inherited by the daughter cell that will remain a stem cell. In asymmetric AP divisions, the daughter cell that maintains stem cell character, rather than that delaminating and assuming a neurogenic fate, is known to inherit the basal process of the mother AP (Konno et al., 2008; Shitamukai et al., 2011; Tsunekawa et al., 2012). We investigated the inheritance of the CR relative to that of the basal process in mitotic APs (Figures 7G–7I).

Most mitotic APs showed asymmetric distribution of the basal process into one daughter cell (Figure 7G). We observed that in AP divisions with such asymmetric basal process inheritance, the majority of the daughter cells that inherited the basal process also inherited the CM (Figure 7I). Such asymmetric coinheritance of CM and basal process was observed for both centrosomal (i.e., CR) and noncentrosomal CM. We conclude that upon asymmetric AP division, the CR is preferentially inherited by the daughter cell that retains stem cell character.

DISCUSSION

In this study, we have shown that CM typically remains attached to the basal body/mother centriole through mitosis at one spindle pole and is asymmetrically inherited by one daughter cell. To our knowledge, such persistence of centriole-attached CM in mitotic somatic cells has not been reported previously.

Our data challenge the generally accepted model in which the primary cilium is completely disassembled prior to mitosis (Garcia-Gonzalo and Reiter, 2012; Kim and Dynlacht, 2013; Kim and Tsiokas, 2011; Seeley and Nachury, 2010). We find that, at the G2-M phase transition, the shortening cilium is actually internalized with the basal body (Figure 7J). Because the basal body/mother centriole maintains its attachment to the remaining CM, it serves a dual function as a basal body as well as a part of one mitotic spindle pole. It was reported recently that *Drosophila* spermatocytes assemble and retain cilia at all centrioles through meiosis, showing that basal body function in nucleating cilia is not incompatible with a function as a spindle pole (Riparbelli et al., 2012).

Previous studies demonstrated that inheritance of the "old" mother centriole is linked to asymmetries in cilium reassembly and ciliary signaling between daughter cells (Anderson and Stearns, 2009; Piotrowska-Nitsche and Caspary, 2012). However, it was unclear which feature of the "old" versus "new" mother centriole is responsible for inducing these asymmetries. Our study identifies the CM as a key structural component of the "old" mother centriole in mitotic cells. Furthermore, we show that CR inheritance by one daughter cell underlies asymmetric ciliary signaling between daughter cells.

Classical studies have demonstrated that ciliogenesis is initiated either by Golgi-derived intracellular CM vesicles docking to the mother centriole or by direct docking of the mother centriole to the plasma membrane (Sorokin, 1962, 1968). Our data uncover a pathway of ciliogenesis that does not involve docking of the older mother centriole to a membrane. Specifically, one of the daughter cells simply inherits the already CM-bearing centriole from the mother cell and thus can directly proceed with cilium outgrowth (Figure 7J, left and middle). In contrast, the other daughter cell inheriting either the new mother centriole or the old mother centriole without CM can proceed with cilium outgrowth only after this centriole has docked to

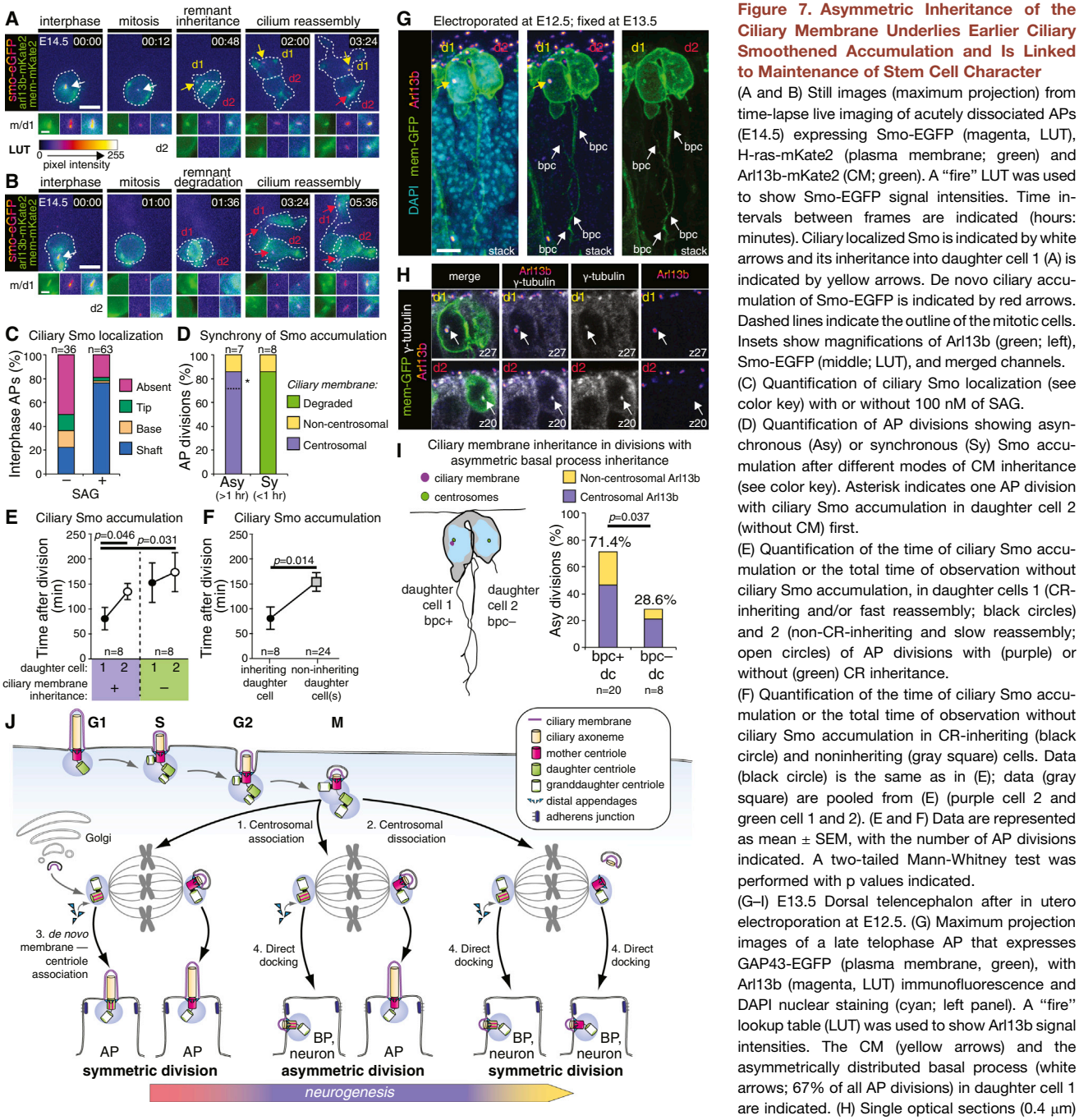

Figure 7. Asymmetric Inheritance of the Ciliary Membrane Underlies Earlier Ciliary Smoothened Accumulation and Is Linked to Maintenance of Stem Cell Character

(A and B) Still images (maximum projection) from time-lapse live imaging of acutely dissociated APs (E14.5) expressing Smo-EGFP (magenta, LUT), H-ras-mKate2 (plasma membrane; green) and Arl13b-mKate2 (CM; green). A "fire" LUT was used to show Smo-EGFP signal intensities. Time intervals between frames are indicated (hours: minutes). Ciliary localized Smo is indicated by white arrows and its inheritance into daughter cell 1 (A) is indicated by yellow arrows. De novo ciliary accumulation of Smo-EGFP is indicated by red arrows. Dashed lines indicate the outline of the mitotic cells. Insets show magnifications of Arl13b (green; left), Smo-EGFP (middle; LUT), and merged channels.

(C) Quantification of ciliary Smo localization (see color key) with or without 100 nM of SAG.

(D) Quantification of AP divisions showing asynchronous (Asy) or synchronous (Sy) Smo accumulation after different modes of CM inheritance (see color key). Asterisk indicates one AP division with ciliary Smo accumulation in daughter cell 2 (without CM) first.

(E) Quantification of the time of ciliary Smo accumulation or the total time of observation without ciliary Smo accumulation, in daughter cells 1 (CR-inheriting and/or fast reassembly; black circles) and 2 (non-CR-inheriting and slow reassembly; open circles) of AP divisions with (purple) or without (green) CR inheritance.

(F) Quantification of the time of ciliary Smo accumulation or the total time of observation without ciliary Smo accumulation in CR-inheriting (black circle) and noninheriting (gray square) cells. Data (black circle) is the same as in (E); data (gray square) are pooled from (E) (purple cell 2 and green cell 1 and 2). (E and F) Data are represented as mean ± SEM, with the number of AP divisions indicated. A two-tailed Mann-Whitney test was performed with p values indicated.

(G–I) E13.5 Dorsal telencephalon after in utero electroporation at E12.5. (G) Maximum projection images of a late telophase AP that expresses GAP43-EGFP (plasma membrane, green), with Arl13b (magenta, LUT) immunofluorescence and DAPI nuclear staining (cyan; left panel). A "fire" lookup table (LUT) was used to show Arl13b signal intensities. The CM (yellow arrows) and the asymmetrically distributed basal process (white arrows; 67% of all AP divisions) in daughter cell 1 are indicated. (H) Single optical sections (0.4 μm) of the AP in (G) show the centrosomes (arrows; γ-tubulin immunofluorescence, gray) and CM (magenta, LUT) in daughter 1 and 2. (I) Quantification of asymmetric AP divisions showing CM inheritance in basal process-inheriting and noninheriting daughters as a percentage of all asymmetrically dividing APs (centrosome-associated CM, purple, 35% of all divisions; noncentrosomal CM, yellow, 16% of all divisions). The cartoon refers to the mitotic AP shown in (G).

(J) Model of the modes of CM and centriole inheritance and the subsequent ciliogenesis pathways in different types of AP divisions. Two possible outcomes exist for the fate of the CM: (1) inheritance into one daughter cell through association with the old mother centriole, followed by apical ciliogenesis; and (2) dissociation of the CM from the old mother centriole, followed by direct docking of the latter to the lateral membrane and basolateral ciliogenesis. For the original daughter centriole that matures into the new mother centriole, two possible outcomes exist: (1) association of a de novo Golgi-derived CM vesicle to this centriole, followed by apical ciliogenesis; and (2) no association of CM, followed by direct docking of this centriole to the lateral membrane and basolateral ciliogenesis. AP, apical progenitor; BP, basal progenitor; bpc, basal process, d1/2, daughter cell 1/2, m, mother cell; mem, membrane. Scale bars, 10 μm (A and B), 2 μm (insets in A and B), and 5 μm (G). See also Figure S6B and Movies S6 and S7.

either an intracellular membrane vesicle (Figure 7J, left) or the plasma membrane (Figure 7J, middle; Sorokin, 1962, 1968).

We reported previously that nascent differentiating daughter cells (basal progenitors, neurons) re-establish a cilium at their basolateral plasma membrane prior to their delamination (Wilsch-Bräuninger et al., 2012). This basolateral ciliogenesis occurs by docking of a centriole to the lateral plasma membrane, whereas apical ciliogenesis in APs typically involves an intracellular CM vesicle. Here, we show that the CR is preferentially inherited by the daughter cell that retains stem cell character. The latter finding provides a plausible mechanistic explanation for the previous observation that elder centrioles versus new centrioles are preferentially inherited by AP versus differentiating daughter cells, respectively (Wang et al., 2009). It is likely that the spatial and temporal asymmetries in cilium reformation between AP daughter cells differentially expose them to signals, such as proliferative signals from the CSF. Therefore, we propose that daughter cells that inherit the CR remain APs (Figure 7J, middle). After division, the membrane of the CR will insert into the apical plasma membrane either by direct exocytosis or by transcytosis from the lateral membrane. In contrast, the centrosome containing the membraneless new mother centriole will directly dock to the lateral membrane to nucleate a basolateral cilium de novo (Figure 7J, middle), and the cell will subsequently delaminate and differentiate.

Given that inheritance of the CR is always an asymmetric event, an important question is whether and how this inheritance is compatible with symmetric divisions. During neurogenesis, two types of symmetric AP division exist. Symmetric proliferative divisions that give rise to two AP daughter cells constitute the principal type of division prior to neurogenesis and decrease in frequency after its onset. In contrast, symmetric neurogenic divisions that give rise to two differentiating daughters cells increase in frequency toward the end of murine neurogenesis.

Specifically, the stage when Arl13b was most frequently detected also at the second centrosome of mitotic APs was the preneurogenic stage when symmetric proliferative divisions prevail. We suggest that this Arl13b immunoreactivity reflects newly synthesized apically destined CM. We propose that in symmetric proliferative divisions, the new mother centriole is able to capture Golgi-derived de novo CM (Figure 7J, left). This membrane capturing can occur already during mitosis, in contrast to the direct docking of the centriole at the plasma membrane that can occur only after mitosis. Because apical Golgi-derived membrane trafficking is downregulated at the onset of neurogenesis (Aaku-Saraste et al., 1997), we propose that APs lose the capacity of capturing Golgi-derived membrane as neurogenesis progresses. Therefore, this property of early neural progenitors is responsible for the earlier ciliogenesis in daughter cells inheriting the new mother centriole in symmetric proliferative divisions at early stages (Figure 7J, left) versus asymmetric (Figure 7J, middle) and symmetric (Figure 7J, right) neurogenic divisions at later stages.

We found that inheritance of CM occurs increasingly in non-centrosomal form as neurogenesis progresses. This leads us to propose that in symmetric neurogenic divisions, both (now membraneless) centrosomes dock at the lateral membrane, and de novo basolateral ciliogenesis occurs in both daughter cells (Figure 7J, right). Subsequently, both daughters delaminate from the ventricular surface and differentiate.

In conclusion, our study uncovers an additional feature of the inherent asymmetries that exist between daughter cells due to the differences in centriole age. Specifically, CR inheritance emerges as an important means of establishing asymmetric behavior between daughter cells.

EXPERIMENTAL PROCEDURES

Further details are provided in the Extended Experimental Procedures.

Mice and In Utero Electroporation

Wild-type C57BL/6 mouse embryos (E9.5–E16.5) were used. APs in E12.5–E15.5 dorsal telencephalon were labeled by in utero electroporation, followed (1) after 1 day by fixation and processing for immunofluorescence, (2) after 5 hr by preparation of organotypic slice cultures, or (3) immediately by preparation of dissociated cell cultures, both for live imaging. All animal studies were conducted in accordance with German animal welfare legislation, and the necessary licenses obtained from the regional Ethical Commission for Animal Experimentation of Dresden, Germany.

Immunofluorescence and Electron Microscopy

Immunofluorescence on sections of paraformaldehyde-fixed dorsal telencephalon and on methanol-fixed cell cultures was performed according to standard methods. E12.5 dorsal telencephalon was analyzed by SBF-SEM and by transmission EM, with pre- or postembedding Arl13b immunolabeling and as combined correlative light and electron microscopy as indicated.

Cell-Surface Biotinylation

For cell-surface biotinylation of the apical plasma membrane of APs, the ventricular surface of E14.5 telencephalon was exposed to a membrane-impermeable, crosslinker-bearing biotin at 4°C, followed by chase at 37°C, fixation, and combined biotin detection/immunofluorescence.

Live Imaging

Cultures of organotypic slices and dissociated cells prepared from dorsal telencephalon and HEK293T cell cultures, expressing various fluorescent protein-tagged markers were subjected to live imaging using 10–15 min time-lapse intervals.

Statistical Analysis

For the data shown in Figures 4F, 6E, 6F, 7E, and 7F, a two-tailed nonparametric Mann-Whitney test was performed using Prism software (GraphPad). For the data shown in Figures 3F, 4E, and 7I, a two-tailed exact binomial probability test assuming normal distribution was performed with a 0.5 random probability for CR inheritance by, or ciliogenesis in, a specific daughter cell by chance. Significance was assumed when $p < 0.05$.

SUPPLEMENTAL INFORMATION

Supplemental Information includes Extended Experimental Procedures, six figures, and seven movies and can be found with this article online at http://dx.doi.org/10.1016/j.cell.2013.08.060.

ACKNOWLEDGMENTS

We are indebted to Jussi Helppi and team of the Animal Facility, Jan Peychl and team of the Light Microscopy Facility, and various other services and facilities of the Max Planck Institute of Molecular Cell Biology and Genetics for outstanding support. We thank Miguel Turrero García for advice on organotypic slice culture, Jula Peters for excellent technical assistance, and Stephan Saalfeld for help with the TrakEM plugin. We acknowledge Michel Bornens, Tamara Caspary, Fumio Matsuzaki, Kirk Mykytyn, and Caren Norden for their kind gift of reagents and thank Alex Sykes and Marnix Wieffer for critical

reading of the manuscript. J.T.M.L.P. was supported by an EMBO long-term fellowship. W.B.H. was supported by grants from the DFG (SFB 655, A2; TRR 83, Tp6) and the ERC (250197), by the DFG-funded Center for Regenerative Therapies Dresden, and by the Fonds der Chemischen Industrie.

Received: January 9, 2013
Revised: June 28, 2013
Accepted: August 27, 2013
Published: October 10, 2013

REFERENCES

Aaku-Saraste, E., Oback, B., Hellwig, A., and Huttner, W.B. (1997). Neuroepithelial cells downregulate their plasma membrane polarity prior to neural tube closure and neurogenesis. Mech. Dev. *69*, 71–81.

Anderson, C.T., and Stearns, T. (2009). Centriole age underlies asynchronous primary cilium growth in mammalian cells. Curr. Biol. *19*, 1498–1502.

Berbari, N.F., Johnson, A.D., Lewis, J.S., Askwith, C.C., and Mykytyn, K. (2008). Identification of ciliary localization sequences within the third intracellular loop of G protein-coupled receptors. Mol. Biol. Cell *19*, 1540–1547.

Cevik, S., Hori, Y., Kaplan, O.I., Kida, K., Toivenon, T., Foley-Fisher, C., Cottell, D., Katada, T., Kontani, K., and Blacque, O.E. (2010). Joubert syndrome Arl13b functions at ciliary membranes and stabilizes protein transport in Caenorhabditis elegans. J. Cell Biol. *188*, 953–969.

Chen, J.K., Taipale, J., Young, K.E., Maiti, T., and Beachy, P.A. (2002). Small molecule modulation of Smoothened activity. Proc. Natl. Acad. Sci. USA *99*, 14071–14076.

Duldulao, N.A., Lee, S., and Sun, Z. (2009). Cilia localization is essential for in vivo functions of the Joubert syndrome protein Arl13b/Scorpion. Development *136*, 4033–4042.

Frank-Kamenetsky, M., Zhang, X.M., Bottega, S., Guicherit, O., Wichterle, H., Dudek, H., Bumcrot, D., Wang, F.Y., Jones, S., Shulok, J., et al. (2002). Small-molecule modulators of Hedgehog signaling: identification and characterization of Smoothened agonists and antagonists. J. Biol. *1*, 10.

Garcia-Gonzalo, F.R., and Reiter, J.F. (2012). Scoring a backstage pass: mechanisms of ciliogenesis and ciliary access. J. Cell Biol. *197*, 697–709.

Goetz, S.C., and Anderson, K.V. (2010). The primary cilium: a signalling centre during vertebrate development. Nat. Rev. Genet. *11*, 331–344.

Götz, M., and Huttner, W.B. (2005). The cell biology of neurogenesis. Nat. Rev. Mol. Cell Biol. *6*, 777–788.

Graser, S., Stierhof, Y.D., Lavoie, S.B., Gassner, O.S., Lamla, S., Le Clech, M., and Nigg, E.A. (2007). Cep164, a novel centriole appendage protein required for primary cilium formation. J. Cell Biol. *179*, 321–330.

Horner, V.L., and Caspary, T. (2011). Disrupted dorsal neural tube BMP signaling in the cilia mutant Arl13b hnn stems from abnormal Shh signaling. Dev. Biol. *355*, 43–54.

Kim, S., and Tsiokas, L. (2011). Cilia and cell cycle re-entry: more than a coincidence. Cell Cycle *10*, 2683–2690.

Kim, S., and Dynlacht, B.D. (2013). Assembling a primary cilium. Curr. Opin. Cell Biol. *25*, 506–511.

Konno, D., Shioi, G., Shitamukai, A., Mori, A., Kiyonari, H., Miyata, T., and Matsuzaki, F. (2008). Neuroepithelial progenitors undergo LGN-dependent planar divisions to maintain self-renewability during mammalian neurogenesis. Nat. Cell Biol. *10*, 93–101.

Kriegstein, A., and Alvarez-Buylla, A. (2009). The glial nature of embryonic and adult neural stem cells. Annu. Rev. Neurosci. *32*, 149–184.

Lancaster, M.A., and Knoblich, J.A. (2012). Spindle orientation in mammalian cerebral cortical development. Curr. Opin. Neurobiol. *22*, 737–746.

Lehtinen, M.K., and Walsh, C.A. (2011). Neurogenesis at the brain-cerebrospinal fluid interface. Annu. Rev. Cell Dev. Biol. *27*, 653–679.

Louvi, A., and Grove, E.A. (2011). Cilia in the CNS: the quiet organelle claims center stage. Neuron *69*, 1046–1060.

Mogensen, M.M., Malik, A., Piel, M., Bouckson-Castaing, V., and Bornens, M. (2000). Microtubule minus-end anchorage at centrosomal and non-centrosomal sites: the role of ninein. J. Cell Sci. *113*, 3013–3023.

Nachury, M.V., Seeley, E.S., and Jin, H. (2010). Trafficking to the ciliary membrane: how to get across the periciliary diffusion barrier? Annu. Rev. Cell Dev. Biol. *26*, 59–87.

Nigg, E.A., and Stearns, T. (2011). The centrosome cycle: Centriole biogenesis, duplication and inherent asymmetries. Nat. Cell Biol. *13*, 1154–1160.

Pelletier, L., and Yamashita, Y.M. (2012). Centrosome asymmetry and inheritance during animal development. Curr. Opin. Cell Biol. *24*, 541–546.

Piotrowska-Nitsche, K., and Caspary, T. (2012). Live imaging of individual cell divisions in mouse neuroepithelium shows asymmetry in cilium formation and Sonic hedgehog response. Cilia *1*, 6.

Reiter, J.F., Blacque, O.E., and Leroux, M.R. (2012). The base of the cilium: roles for transition fibres and the transition zone in ciliary formation, maintenance and compartmentalization. EMBO Rep. *13*, 608–618.

Riparbelli, M.G., Callaini, G., and Megraw, T.L. (2012). Assembly and persistence of primary cilia in dividing Drosophila spermatocytes. Dev. Cell *23*, 425–432.

Robbins, D.J., Fei, D.L., and Riobo, N.A. (2012). The Hedgehog signal transduction network. Sci. Signal. *5*, re6.

Rohatgi, R., Milenkovic, L., and Scott, M.P. (2007). Patched1 regulates hedgehog signaling at the primary cilium. Science *317*, 372–376.

Seeley, E.S., and Nachury, M.V. (2010). The perennial organelle: assembly and disassembly of the primary cilium. J. Cell Sci. *123*, 511–518.

Shitamukai, A., Konno, D., and Matsuzaki, F. (2011). Oblique radial glial divisions in the developing mouse neocortex induce self-renewing progenitors outside the germinal zone that resemble primate outer subventricular zone progenitors. J. Neurosci. *31*, 3683–3695.

Sillibourne, J.E., Specht, C.G., Izeddin, I., Hurbain, I., Tran, P., Triller, A., Darzacq, X., Dahan, M., and Bornens, M. (2011). Assessing the localization of centrosomal proteins by PALM/STORM nanoscopy. Cytoskeleton *68*, 619–627.

Sorokin, S. (1962). Centrioles and the formation of rudimentary cilia by fibroblasts and smooth muscle cells. J. Cell Biol. *15*, 363–377.

Sorokin, S.P. (1968). Reconstructions of centriole formation and ciliogenesis in mammalian lungs. J. Cell Sci. *3*, 207–230.

Tsunekawa, Y., Britto, J.M., Takahashi, M., Polleux, F., Tan, S.S., and Osumi, N. (2012). Cyclin D2 in the basal process of neural progenitors is linked to non-equivalent cell fates. EMBO J. *31*, 1879–1892.

Wang, X., Tsai, J.W., Imai, J.H., Lian, W.N., Vallee, R.B., and Shi, S.H. (2009). Asymmetric centrosome inheritance maintains neural progenitors in the neocortex. Nature *461*, 947–955.

Wilsch-Bräuninger, M., Peters, J., Paridaen, J.T., and Huttner, W.B. (2012). Basolateral rather than apical primary cilia on neuroepithelial cells committed to delamination. Development *139*, 95–105.

Yamashita, Y.M., Mahowald, A.P., Perlin, J.R., and Fuller, M.T. (2007). Asymmetric inheritance of mother versus daughter centrosome in stem cell division. Science *315*, 518–521.